Mutant ELOVL4 That Causes Autosomal Dominant Stargardt-3 Macular Dystrophy Is Misrouted to Rod Outer Segment Disks

Martin-Paul Agbaga,[1,2] Beatrice M. Tam,[4] Jenny S. Wong,[4] Lee Ling Yang,[4] Robert E. Anderson,[1–3] and Orson L. Moritz[4]

[1]Department of Ophthalmology, University of Oklahoma Health Sciences Center, Oklahoma City, Oklahoma, United States
[2]Dean McGee Eye Institute, Oklahoma City, Oklahoma, United States
[3]Department of Cell Biology, University of Oklahoma Health Sciences Center, Oklahoma City, Oklahoma, United States
[4]Department of Ophthalmology and Vancouver Eye Care Center, University of British Columbia, Vancouver, Canada

Correspondence: Martin-Paul Agbaga, Department of Ophthalmology, University of Oklahoma Health Sciences Center, 608 Stanton L. Young Boulevard, DMEI 429PB, Oklahoma City, OK 73104, USA; martin-paul-agbaga@ouhsc.edu.

Orson L. Moritz, Department of Ophthalmology and Visual Sciences, UBC/VGH Eye Care Centre, 2550 Willow Street, Vancouver, BC, Canada V5Z 3N9; olmoritz@mail.ubc.ca.

Submitted: August 20, 2013
Accepted: April 27, 2014

Citation: Agbaga M-P, Tam BM, Wong JS, Yang LL, Anderson RE, Moritz OL. Mutant ELOVL4 that causes autosomal dominant Stargardt-3 macular dystrophy is misrouted to rod outer segment disks. *Invest Ophthalmol Vis Sci*. 2014;55:3669–3680. DOI:10.1167/iovs.13-13099

Purpose. Autosomal dominant Stargardt macular dystrophy caused by mutations in the Elongation of Very Long Chain fatty acids (*ELOVL4*) gene results in macular degeneration, leading to early childhood blindness. Transgenic mice and pigs expressing mutant ELOVL4 develop progressive photoreceptor degeneration. The mechanism by which these mutations cause macular degeneration remains unclear, but have been hypothesized to involve the loss of an ER-retention dilysine motif located in the extreme C-terminus. Dominant negative mechanisms and reduction in retinal polyunsaturated fatty acids also have been suggested. To understand the molecular mechanisms involved in disease progression in vivo, we addressed the hypothesis that the disease-linked C-terminal truncation mutant of ELOVL4 exerts a dominant negative effect on wild-type (WT) ELOVL4, altering its subcellular localization and function, which subsequently induces retinal degeneration and loss of vision.

Methods. We generated transgenic *Xenopus laevis* that overexpress HA-tagged murine ELOVL4 variants in rod photoreceptors.

Results. Tagged or untagged WT ELOVL4 localized primarily to inner segments. However, the mutant protein lacking the dilysine motif was mislocalized to post-Golgi compartments and outer segment disks. Coexpression of mutant and WT ELOVL4 in rods did not result in mislocalization of the WT protein to outer segments or in the formation of aggregates. Full-length HA-tagged *ELOVL4* lacking the dilysine motif (K308R/K310R) necessary for targeting the WT ELOVL4 protein to the endoplasmic reticulum was similarly mislocalized to outer segments.

Conclusions. We propose that expression and outer segment mislocalization of the disease-linked 5–base-pair deletion mutant ELOVL4 protein alters photoreceptor structure and function, which subsequently results in retinal degeneration, and suggest three possible mechanisms by which mutant ELOVL4 may induce retinal degeneration in STGD3.

Keywords: autosomal dominant Stargardt-like macular dystrophy (STGD3), elongation of very long chain fatty acids-4 (ELOVL4), retinal degeneration, photoreceptor outer segment

Juvenile-onset autosomal dominant Stargardt macular dystrophy (STGD3) is caused by frame-shift mutations in elongation of very long chain fatty acids-4 *(ELOVL4)*.[1] *ELOVL4* encodes a transmembrane protein that catalyzes the initial rate-limiting condensation reaction in very long chain fatty acid biosynthesis.[2,3] The disease-causing mutations alter the c-terminal coding sequence, including deletion of a predicted dilysine endoplasmic reticulum (ER) retention motif. Tissue culture studies indicate that the mutant ELOVL4 can exert dominant negative effects on wild-type (WT) ELOVL4, misrouting it from the ER to Golgi membranes or aggresomes.[4–7] Also, in cultured cells, mutant ELOVL4 cannot synthesize very long chain polyunsaturated fatty acids (VLC-PUFA) and inhibits the biosynthetic ability of WT ELOVL4.[8]

Unlike cultured cells, photoreceptors sort nascent transmembrane proteins into at least four major membrane compartments: plasma, outer segment (OS) disk, inner segment (IS), and synaptic membranes. Furthermore, aggresomes have not been observed in photoreceptors and are only found in cells that express intermediate filament proteins.[9] Hence, it is unclear whether mislocalization of WT ELOVL4 by truncated mutant ELOVL4 occurs in photoreceptors.

Several mouse models of STGD3 expressing mutant ELOVL4 develop slow, progressive retinal degeneration (RD) and have reduced VLC-PUFA.[10–14] In vivo, the WT ELOVL4 protein is localized within photoreceptor outer nuclear layer and ISs without any OS or synaptic terminal labeling.[7,15,16] Grayson and Molday[7] also reported expression of ELOVL4 in ganglion cells in human retina. However, photoreceptor-specific expression of fluorescent-tagged mutant ELOVL4 results in disorganized IS and OS membranes and subsequent photoreceptor dysfunction in pigs.[17] In mutant *Elovl4* knockin mice, the

mutant ELOVL4 was reportedly mislocalized to dendrites of bipolar cells.[18] Collectively, these studies suggest that RD is due to expression and mislocalization of mutant ELOVL4 protein or its inhibition of VLC-PUFA biosynthesis. Thus, dominant negative mechanisms and reduced VLC-PUFA are possible causes of RD. Heterozygous *Elovl4* mice develop normal photoreceptors that do not degenerate, suggesting haploinsufficiency is not the cause of RD.[19,20]

Here, we tested the hypothesis that the disease-linked C-terminal truncated ELOVL4 exerts a dominant negative effect on WT ELOVL4 to form aggregates that are misrouted to wrong intracellular compartments of photoreceptors. Expression and accumulation of such aggregates could eventually cause cell death. We generated *Xenopus laevis* that overexpressed hemagglutinin (HA)-tagged murine ELOVL4 variants in rods driven by the *X. laevis* rod opsin promoter and assessed expression, subcellular localization, and photoreceptor integrity. We also compared intracellular localizations of mislocalized mutant ELOVL4 with a mislocalized rhodopsin mutant (Q344ter) responsible for RP.[21]

We show that WT ELOVL4 localized to rod IS of *X. laevis*. Surprisingly, mutant ELOVL4 was misrouted from IS through the Golgi to rod OS membranes. However, unlike localization-defective mutants in rhodopsin, there was no mislocalization to other compartments, such as IS lateral plasma membrane or synaptic region plasma membranes. When coexpressed, mutant, but not WT ELOVL4, was misrouted to Golgi and OS disks. We established that the C-terminal dilysine motif is necessary for proper localization of ELOVL4 to IS. Thus, RD in STGD3 patients is likely due to mislocalization of the mutant ELOVL4 coupled with the mutant's inhibitory effect on the WT's ability to make VLC-PUFA.

Materials and Methods

Transgene Expression Constructs

All transgenes used for expression of the various ELOVL4 fusion proteins in *X. laevis* photoreceptors were based on pXOP-2DI attb enhanced green florescent protein (eGFP) vector.[22] The green fluorescent protein (GFP) cDNA downstream of the *X. laevis* opsin promoter in the pXOP-2DI attb eGFP vector was excised with EcoRI and NotI and replaced with PCR-generated products of the various *Elovl4* HA epitope tagged (YPYDVPDYA) at the N-terminus of the *Elovl4*, or untagged constructs using infusion cloning reactions (Clontech, Mountain View, CA, USA). Each construct contained Kozak translation initiation and stop codons to ensure proper expression. The rhodopsin mutant (Q344ter) and the bovine rhodopsin GFP-tagged protein construct variants have been described previously.[21,23] All PCR products and site-directed mutagenesis were achieved using Phusion High-Fidelity PCR master mix with HF Buffer (New England Biolabs, Beverly, MA, USA). The transgene constructs were verified by sequencing. For transgenesis, expression vectors were linearized with FseI (New England Biolabs) and purified using Qiagen QIAquick gel extraction kit (Qiagen Sciences, Valencia, CA, USA).

Generation and Rearing of Transgenic *X. laevis*

Transgenic *X. laevis* tadpoles were generated using methods described previously,[9,21,22,24,25] and the embryos were housed in 4-L tanks at 18°C in a 12-hour light/dark cycle incubator. Double-transgenic animals were generated by simultaneous injection of two transgene constructs. G418 selection of transgenic tadpoles was initiated 24 hours post fertilization for 96 hours.[9,22,25] Normally developed tadpoles were selected and killed at 14 days postfertilization (dpf). One eye from each tadpole was enucleated and fixed overnight in 4% formaldehyde in 0.1 M sodium phosphate buffer (pH 7.4) for immunohistochemistry analyses, while the other eye was solubilized and used for Western and dot blot analyses.[9,21,26,27] For dot blot analyses, 20 to 30 animals were generated and analyzed for each transgene.

Immunohistochemistry and Confocal Microscopy

The fixed enucleated eyes were cryoprotected by infiltration with 20% sucrose solution in 0.1 M sodium phosphate buffer (pH 7.4), embedded in Tissue-Tek O.C.T. compound (Sakura Finetek, Torrance, CA, USA), and frozen. Retinal cryosections (12 μm) were cut, collected on Fisherbrand Superfrost/Plus microslides (Thermo Fisher Scientific, Waltham, MA, USA), and stored at −20°C until used.[9,28] For confocal microscopy analyses, the retinal sections were labeled with HA monoclonal antibody (1:1000) (Cedarlane, Burlington, ON, Canada), anticalnexin at 1:50 dilution (Stressgen Biotechnologies, Victoria, BC, Canada), or previously characterized affinity-purified ELOVL4 (1:200) polyclonal antibodies[16] followed by a 1:750 dilution of Cy3-labeled secondary antibody (Jackson ImmunoResearch, West Grove, PA, USA). Confocal microscopy results are based on detailed observations of at least five transgenic animals per transgene, with at least four sections examined per animal. For some transgenes, additional sets of four or more sections were labeled with alternate labeling procedures. The total numbers of animals examined with each labeling procedure is given as "*n*" in figure legends. The affinity-purified custom rabbit ELOVL4 polyclonal antibodies were generated from synthetic 12-amino acid peptide (GKPQKNGKPKGE) corresponding to amino acids 301 to 312 of the mouse ELOVL4 protein. This antibody is able to recognize WT ELOVL4 but not the mutant ELOVL4 that loses these amino acids used in making the antibodies. The specificity of the ELOVL4 antibody to recognize the mouse ELOVL4 protein was determined by Western blot on protein lysates from mouse *Elovl4* mini-gene–transfected human embryonic kidney (HEK) cells, mouse and rat retina, brain, and skin tissues that express the ELOVL4 protein. The affinity-purified ELOVL4 recognized approximately 32-kDa protein, which was specifically blocked by antigenic peptides used in making the antibodies[16] and is consistent with previously published ELOVL4 antibodies.[7,15] To further confirm the specificity of the ELOVL4 antibodies, *Elovl4* mini-gene tagged with triple HA at the N-terminus was transfected into HEK cells. Protein lysates from the HA-tagged *Elovl4* transfected HEK cells were resolved on SDS-PAGE gels, transferred to nitrocellulose membrane, and probed with either HA or ELOVL4 antibodies. Both HA and ELOVL4 antibodies recognize the same molecular weight protein on the blots confirming the specificity of the ELOVL4 antibodies.[8] Monoclonal antibodies 2B2[29] and B630N[30] were used to label mutant human Q344ter rhodopsin and endogenous *X. laevis* rhodopsin, respectively, as previously described.[31] Wheat germ agglutinin (WGA) conjugated to Alexa Fluor 488 or 555 diluted 1:200 (Invitrogen, Grand Island, NY, USA) was used to label photoreceptor membranes and Hoescht 33342 (10 μg/mL) (Sigma-Aldrich, St. Louis, MO, USA) was used to label nuclei. Confocal images were acquired using a Zeiss 510 Meta laser scanning confocal microscope (Carl Zeiss, Peabody, MA, USA)[21,27,28] using a ×40 numerical aperture (NA) 1.4 water immersion objective. Using Zeiss imaging software, we collected red, green, blue (RGB) images in which each channel represented a different label. Each channel was then independently adjusted using Adobe Photoshop (Adobe Systems, Inc., San Jose, CA, USA).

Investigative Ophthalmology & Visual Science

Antibody labeling was adjusted linearly. WGA labeling was adjusted nonlinearly to emphasize fainter labeling of IS membranes. Images were assembled into figures and annotated using Adobe Photoshop.

Results

Differential Subcellular Localization of WT and Mutant ELOVL4 Proteins in *X. laevis* Rod Photoreceptors

To determine the relative localization of WT and mutant ELOVL4 independently in vivo, we took advantage of the large photoreceptors of *X. laevis* within which photoreceptor organelles and structures can be easily imaged and tracked by confocal microscopy.[32] We generated transgenic *X. laevis* that overexpressed murine untagged WT ELOVL4, HA-tagged WT ELOVL4 (HA-WT ELOVL4), and HA-tagged disease-linked 5-bp-deletion (797–801–del_AACTT) mutant ELOVL4 (HA-Mutant ELOVL4) proteins under control of the *X. laevis* rod opsin promoter. We used an HA tag rather than a GFP tag because of the potential for differences in protein biosynthesis and function in GFP-tagged fusion proteins.[33,34] Also, previous studies from our laboratory had shown that HA-tagged murine ELOVL4 was enzymatically active.[8,35] We assessed expression, subcellular protein localization, and photoreceptor integrity by Western and dot blots, immunolabeling, and confocal microscopy. Untagged WT ELOVL4 and HA-ELOVL4 localized to rod IS of *X. laevis* rod photoreceptors, as expected based on previously described ELOVL4 localization experiments in rodent and human photoreceptors (Figs. 1A, 1B).[2,7,15] Within IS, ELOVL4 and HA-ELOVL4 labeling showed negative staining of membrane compartments that were positively stained with WGA. WGA staining is specific for an N-acetyl glucosamine modification of glycoproteins that occurs in the Golgi, and therefore stains Golgi and secretory pathway compartments beyond the Golgi. WGA labeling of internal membranes in ISs is largely coincident with the trans-Golgi marker rab6 (Fig. 2E), indicating that most of this labeling represents Golgi.[36] HA-ELOVL4 labeling was coincident with calnexin labeling (Fig. 2A), indicating that it was localized to the ER, and did not colocalize with the trans-Golgi marker rab6 (Fig. 2C), indicating that it did not enter the Golgi. There was no difference in the localization of untagged WT ELOVL4 (Fig. 1A) and HA-tagged WT ELOVL4 (Fig. 1B), suggesting that the HA tag had no effect on the localization of the ELOVL4 protein. Within the retina, WT and HA-tagged ELOVL4 were observed only in rod photoreceptors, and not in other retinal cell layers.

We then investigated the effect of the 5-bp deletion mutation responsible for Stargardt disease on the localization of HA-tagged ELOVL4. Instead of exclusive IS localization, HA-Δ5-ELOVL4 was also misrouted to OS membranes (Fig. 1C). Within IS, HA-Δ5-ELOVL4 labeling did not negatively stain WGA-positive membranes, and was not entirely coincident with calnexin labeling (Fig. 2B), indicating that it was localized to both ER and other membranes of the biosynthetic pathway, including Golgi, which was confirmed by colocalization of HA-Δ5-ELOVL4 and rab6 (Fig. 2D). Punctate aggregates similar to those previously observed in cell culture experiments were not present.[4–7,37] Furthermore, the mislocalization of HA-Δ5-ELOVL4 (Fig. 1C) was distinct from mislocalization of a rhodopsin variant (Q344ter) that lacks any localization information.[21,33] First, although substantial quantities of HA-Δ5-ELOVL4 were misrouted to OS, significant amounts of it were retained within IS membranes relative to transgenic Q344Ter rhodopsin (Figs. 1C–E). Second, whereas rhodopsin Q344ter was present in OS and IS membranes, including lateral IS plasma membranes, and synaptic region plasma membranes[21] (Fig. 1D), HA-Δ5-ELOVL4 was apparent only in OS membranes and internal IS membranes.

To determine whether HA-Δ5-ELOVL4 protein was present in the OS plasma membrane, and to confirm its absence from lateral plasma membrane and synaptic region plasma membrane, we used detergent-free labeling to accentuate plasma membrane labeling relative to intracellular labeling. We labeled HA-Δ5-ELOVL4 and rhodopsin Q344Ter transgenic retinas in the presence and absence of TX-100 detergent, using monoclonal antibodies that bind predicted extracellular epitopes (Figs. 3A–C). In the absence of detergent, we did not observe any significant OS labeling of HA-Δ5-ELOVL4 (Figs. 3A, 3B), or significant labeling of plasma membrane in any region of the cells. In contrast, the absence of detergent dramatically accentuated Q344Ter rhodopsin plasma membrane labeling, including lateral plasma membrane and synaptic region plasma membrane (Fig. 3C). We concluded that HA-Δ5-ELOVL4 was not efficiently transported to photoreceptor plasma membranes. These results indicate that, although HA-Δ5-ELOVL4 was misrouted from IS ER membranes, it did not exhibit nonspecific mislocalization (Fig. 1D). Rather, HA-Δ5-ELOVL4 is largely confined to the ER, Golgi, and OS disks, and is excluded from all photoreceptor plasma membranes (Fig. 1C).

Effect of Mutant ELOVL4 on the Localization of WT ELOVL4 in Photoreceptors

In cell culture experiments, mutant ELOVL4 is reported to interact with WT ELOVL4 and misroute it from the ER to form mislocalized aggregates.[4–7,37] We reasoned that if HA-Δ5-ELOVL4 interacted with WT ELOVL4, then it might carry WT ELOVL4 protein to the OS and possibly into the phagosomes of the RPE cells. To address this hypothesis, we coexpressed HA-Δ5-ELOVL4 and untagged WT ELOVL4 in transgenic *X. laevis* rods. The motif recognized by the antibody used to label untagged WT ELOVL4 binds within the C-terminus, and therefore does not bind HA-Δ5-ELOVL4.[16] When we coexpressed the HA-Δ5-ELOVL4 and untagged WT ELOVL4 in rods, the WT ELOVL4 localized properly to the IS (Figs. 4A, 4C), while a portion of the HA-Δ5-ELOVL4 protein was again misrouted from the IS to OS (Figs. 4A, 4B). Expression of HA-Δ5-ELOVL4 did not cause mislocalization of WT ELOVL4 protein to OS membranes (Fig. 4C). Again, we did not observe any protein aggregates as previously seen in cultured cells.[6–8,37] Although we cannot rule out the possibility of undetectable levels of WT ELOVL4 mislocalization, our findings suggest that, in vivo, rod photoreceptors independently sort mutant and WT ELOVL4 to different cellular compartments.

The Effect of the Carboxy-Terminal ER Retention/Retrieval Dilysine Motif (KXKXX) on IS Localization of the ELOVL4 Protein

We wished to confirm that OS localization of mutant ELOVL4 was due to absence of the dilysine motif and not some other change (such as a conformational change). We generated a construct consisting of full-length HA-WT ELOVL4 protein in which we mutated the lysine residues of the KPKGE motif to arginine (K308R/K310R). This HA-ELOVL4-KK-RR protein was misrouted to OS of *X. laevis* rod photoreceptors in a manner indistinguishable from the HA-Δ5-ELOVL4 protein (Fig. 5A). This result indicates that loss of the ER retention signal caused misrouting of the HA-Δ5-ELOVL4, including misrouting to OS. Although the HA-ELOVL4-KK-RR was delivered to the OS,

Investigative Ophthalmology & Visual Science

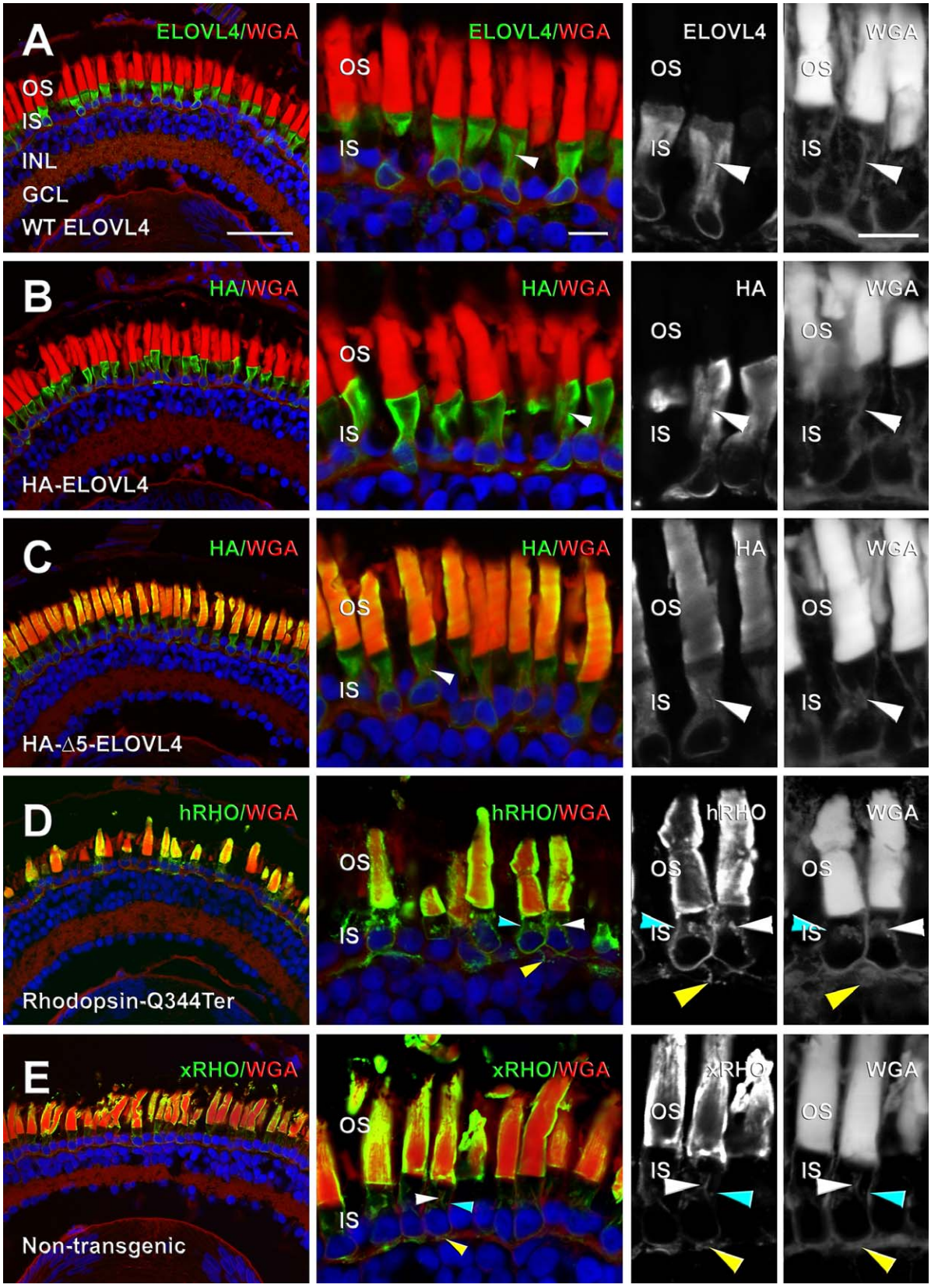

Figure 1. Confocal images of transgenic *X. laevis* rod photoreceptors expressing WT ELOVL4 (untagged), HA-tagged WT ELOVL4, HA tagged mutant ELOVL4, and rhodopsin-Q344Ter transgenes. (**A**, **B**) Merged confocal images of untagged WT-ELOVL4 signal ([**A**] ELOVL4: *green*, $n = 5$) or HA-tagged WT ELOVL4 ([**B**] HA: *green*, $n = 8$), Texas-Red WGA (*red*) and Hoechst 33342 dye (Nuclei, *blue*). WT-ELOVL4 and HA-ELOVL4 were identically exclusively localized to rod photoreceptor IS membranes, but excluded from WGA-positive internal membranes of the IS (*white arrowhead*). WT-ELOVL4 and HA-ELOVL4 were not found within OSs, inner nuclear layer (INL), or ganglion cell layer (GCL). (**C**) HA-Δ5-ELOVL4 (HA: *green*, $n = 19$) was misrouted from rod IS membranes to WGA-positive internal membranes of the IS (*white arrowhead*) and OS membranes.

Investigative Ophthalmology & Visual Science

Colocalization of *red* and *green* signals appears *yellow/orange*. (**D**) Human rhodopsin-Q344Ter labeled with anti-rhodopsin monoclonal antibody 2B2 (hRho: *green*, $n = 5$) was found in rod OS, WGA-positive internal membranes (*white arrowhead*), lateral plasma membrane (*blue arrowhead*), and synaptic region plasma membrane (*yellow arrowhead*). (**E**) WT *X. laevis* rhodopsin labeled with monoclonal antibody B630N (xRho: *green*, $n = 3$) in *X. laevis* rod photoreceptors. *Arrowheads* as in (**D**). *Grayscale* images represent nonmerged WGA or antibody signals shown at higher magnification. *White arrowheads* = WGA-positive internal membranes. *Blue arrowheads* = plasma membrane. *Yellow arrowheads* = synaptic region plasma membranes. *Scale bar*: 50 μm (*left*), 10 μm (*middle*), 10 μm (*grayscale*).

unlike HA-Δ5-ELOVL4 (Fig. 2D), it was not prominent in internal WGA-positive IS membranes, possibly indicating some degree of misfolding.

To confirm the role of the dilysine motif in ELOVL4 localization, we generated a construct in which we restored the ER retention signal to the HA-Δ5-ELOVL4 protein. The last 12 amino acid residues (GKPQKNGKPKGE) from the carboxyl terminus of murine WT ELOVL4 protein containing the dilysine motif, KXKXX, were added to HA-Δ5-ELOVL4 (HA-Δ5-ELOVL4-ERS) and expressed in *X. laevis* rod photoreceptors. This 12 amino acid sequence, which contains the ER retention signal KXKXX, completely restored normal ER localization of the mutant ELOVL4 despite the absence of almost 39 amino acid residues normally found in the WT ELOVL4 protein (Fig. 5B). This further supports the hypothesis that OS mislocalization of HA-Δ5-ELOVL4 is due to loss of the ER retention signal **KXKXX**.

The Effect of Carboxy-Terminal ER Retention/Retrieval Dilysine Motif (KXKXX) on ER Localization of Other Transmembrane Proteins

Many OS-targeted proteins such as rhodopsin, photoreceptor-specific retinol dehydrogenase, and RDS/peripherin have OS targeting signals. Others, such as GTPase-activating complex anchoring protein R9AP, are targeted to the OS by non–sequence-specific transmembrane domains.[21–23,26,38] These signals are required for exclusive OS localization, and in their absence, proteins are indiscriminately targeted to other membranes in addition to OS. Similarly, IS and cellular organelle–designated proteins, such as microsomal membrane resident cytochrome b5 and mitochondrial membrane–targeted antiapoptotic protein BclXL, contain C-terminal located single-pass transmembrane domains, flanked by positively charged residues (in the case of BclXL protein) that target them to ER or mitochondrial membranes, respectively.[33] Modification of these domains or charged residues in these proteins result in default OS mislocalization of these non-OS–targeted proteins in frog rods.[33] Furthermore, studies have demonstrated that juxtaposed dilysine residues at the carboxyl terminus of transmembrane proteins provide a signal to allow retrieval of ER-resident proteins.[39] Our studies (above) have established that the **KPKGE** motif is necessary and sufficient for ER retention of ELOVL4, and that lack of this motif results in OS membrane targeting and probably contributes to subsequent RD. If so, this motif also should be able to redirect OS-localized transmembrane proteins, such as rhodopsin to the IS. To test this hypothesis, we generated four constructs based on rho-GFP, a fusion of bovine rhodopsin (rho) and GFP previously described.[34] These included the following:

1. A Rho-GFP tagged protein lacking the C-terminal OS targeting signal of rhodopsin, VXPX (*Rho-GFPΔCT*),
2. A construct in which we added the last 12 amino acids containing the ELOVL4 ER retention/retrieval signal GKPQKNGKPKGE (ERS) downstream of the *Rho-GFPΔCT* construct to generate *Rho-GFPΔCT-ERS,*
3. A construct with ERS signal following the rhodopsin OS targeting signal, VXPX (CT) (*Rho-GFP-CT-ERS*), and
4. A construct in which the ERS was flanked by rhodopsin OS targeting signals VXPX motif (*Rho-GFP-CT-ERS-CT*).[23,38,40]

We generated transgenic *X. laevis* tadpoles using each of these constructs and determined the localization of the GFP fusion proteins. In transgenic *X. laevis*, the bovine Rho-GFPΔCT protein lacking the OS targeting signal was not only localized to OS, but also mislocalized to IS membranes, including the lateral plasma membrane and synaptic region plasma membrane, as previously described,[34] and was notably absent from ER membranes (Figs. 6A, 6B), similar to rhoQ344ter (Fig. 1). However, when we added the ELOVL4 ERS (KXKXX) membrane localization signal to the Rho-GFPΔCT to generate *Rho-GFPΔCT-ERS*, the resultant fusion protein was completely redirected to the ER membranes of the IS without any OS plasma membrane, synaptic localization, or localization to WGA-positive Golgi and post-Golgi membranes of the IS (Fig. 6C). Moritz et al.[34] developed a Rho-GFP+VXPX (Rho-GFP-CT) construct that has many biochemical properties of rhodopsin and is sorted and targeted like native rhodopsin in *X. laevis* rod photoreceptors (Fig. 6A). We asked whether the ELOVL4 ERS sequence would redirect Rho-GFP-CT (Fig. 6A) from OS to the IS membranes when expressed as *Rho-GFP-CT-ERS*. As predicted, addition of the ELOVL4 ERS retention signal downstream of the VXPX motif completely overrode rhodopsin OS targeting information and caused retention of *Rho-GFP-CT-ERS* fusion protein in IS membranes (Fig. 6D) similar to that observed for *Rho-GFPΔCT-ERS*. We then asked if the ELOVL4 ERS motif is capable of functioning at positions other than the extreme carboxyl terminus of the protein. We therefore added the VXPX motif downstream of the ELOVL4 ERS motif. This was sufficient to redirect the resulting *Rho-GFP-CT-ERS-CT* fusion protein to OS membranes (Fig. 6E). These findings confirm that the ELOVL4 ERS signal KXKXX is a *bonafide* ER retention signal, and must be located at the extreme carboxyl terminal of the protein.

Transgenic Expression of Murine *Elovl4* Variants and Retinal Degeneration in *X. laevis* Photoreceptors

Previous studies have shown that transgenic expression of mutant ELOVL4 induces RD[17] and accumulation of lipofuscin and A2E in mouse models of STGD3.[10] Therefore, we determined the effect of expression of ELOVL4 variants on retinal morphology in *X. laevis* rod photoreceptors. In confocal images, RD was observed in a small subset of animals expressing each ELOVL4 variant (Figs. 7C–J). We quantified rod loss in HA-ELOVL4 versus HA-Δ5-ELOVL4 animals using a dot blot assay for rod opsin as previously described[31] (Fig. 7A). The differences were not statistically significant, indicating that neither construct was dramatically more toxic than the other, although significant toxicity was observed using a previously characterized positive control (human N15S rhodopsin[31]) ($P = 0.008$, $n = 22$ per group, Kruskal-Wallace followed by multiple comparisons according to Conover[41]). Relative to our previous studies involving rhodopsin mutants, ELOVL4 variants caused RD in a much smaller proportion of animals[9,27,42–44] and RD was observed by histology in no more than three animals for

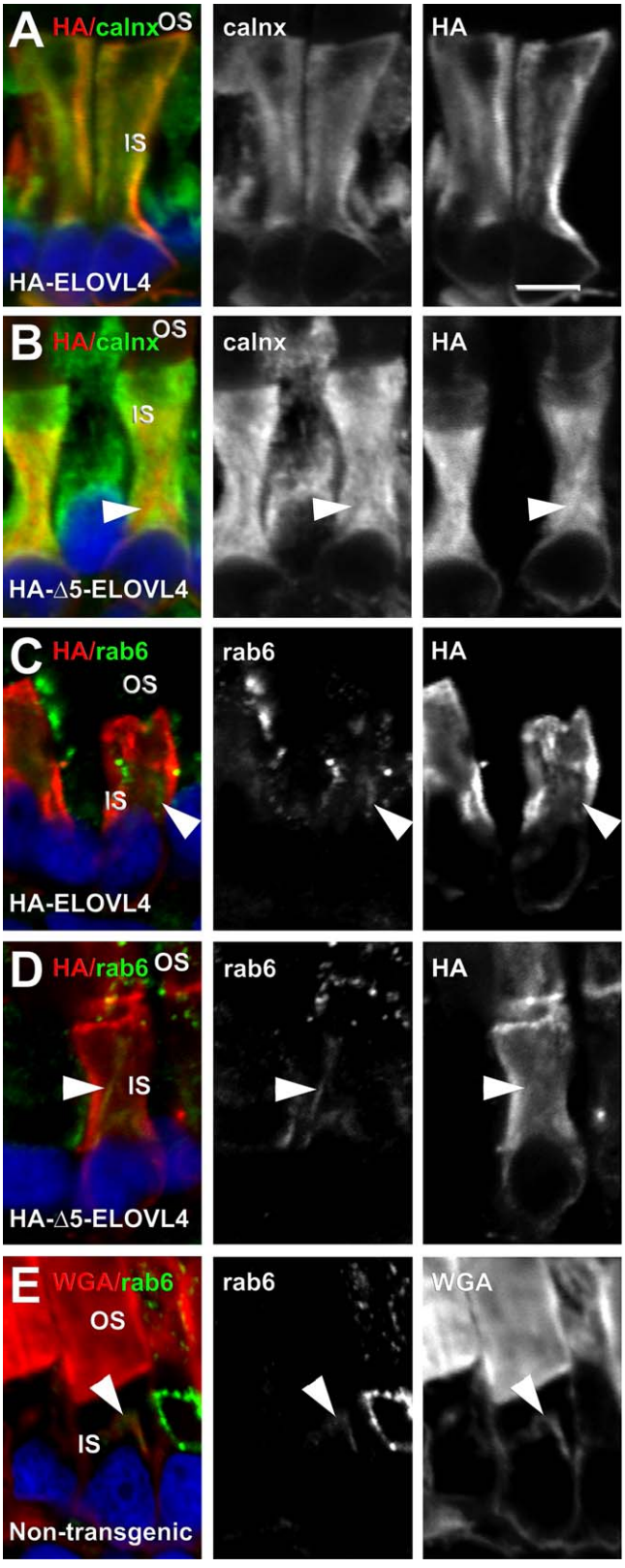

Figure 2. Colocalization of the ER marker calnexin, and Golgi compartment marker rab6, with HA-ELOVL4 and HA-Δ5-ELOVL4 in rod photoreceptor cells. (**A**) Colocalization of HA-ELOVL4 and ER marker calnexin (HA: *red*, calnx: *green*, $n = 3$) within IS membranes of *X. laevis* rod photoreceptors. Note complete overlap of calnexin and HA-ELOVL4 signal. (**B**) Colocalization of HA-Δ5-ELOVL4 and calnexin ($n = 3$). Note partial overlap of calnexin and HA-Δ5-ELOVL4 signals. *Arrowhead* (**B**) indicates region of nonoverlap (HA-positive, calnexin negative). (**C**) Lack of colocalization of HA-ELOVL4 and Golgi marker, rab6 (HA: *red*, rab6: *green*, $n = 3$) within rod photoreceptor IS membranes. HA-ELOVL4 and rab6 do not colocalize. *Arrowhead* indicates HA-negative, rab6-positive membranes. (**D**) Colocalization of HA-Δ5-ELOVL4 and rab6 (HA: *red*, rab6: *green*, $n = 3$). HA-Δ5-ELOVL4 is misrouted to Golgi compartments resulting in significant overlap with rab6 within IS membranes of rod photoreceptor cells (*arrowhead*). (**E**) Colocalization of WGA and rab6 labeling ($n = 3$) in internal membranes of WT rod ISs. The signals are largely coincident within internal membranes of the IS (*arrowhead*), indicating that most of these membranes are Golgi. *Grayscale* images show the indicated isolated signals. *Scale bars*: 5 μm.

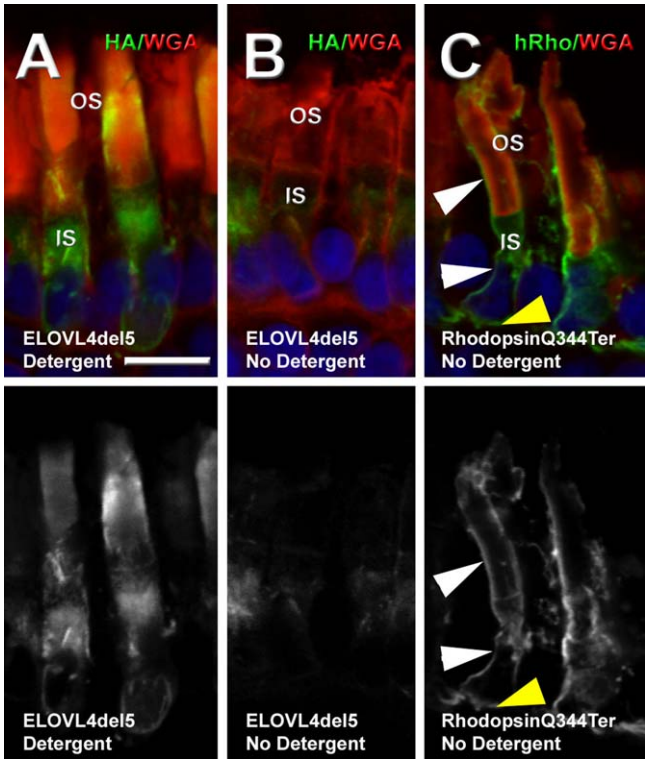

Figure 3. HA-Δ5-ELOVL4 is partially delocalized to the OS, but not to plasma membrane and synaptic terminals. (**A**, **B**) Confocal micrographs of transgenic *X. laevis* rod photoreceptors expressing HA-Δ5-ELOVL4 ([**A**] HA: *green*, $n = 3$) labeled in the presence of detergent that reveals delocalization of HA-Δ5-ELOVL4 to OS without prominent plasma membrane labeling. (**B**) In absence of detergent, there is no observable OS or plasma membrane localization for HA-Δ5-ELOVL4 (HA: *green*, $n = 3$). (**C**) In contrast, in the absence of detergent, 2B2-labeling shows prominent delocalization of Rhodopsin-Q344Ter (hRho: *green*, $n = 3$) to OS and lateral plasma membranes (*white arrowheads*) and synaptic region plasma membrane (*yellow arrowhead*) of rod photoreceptors. In all images, nuclei were stained with Hoescht 33342 and photoreceptor membranes were labeled with WGA (*red*). *Scale bar*: 10 μm.

any given construct. Retinas with RD always had intense HA signal, indicating RD was likely caused by high-level transgene expression.

Effect of Outer Segment Mislocalization of Histidine-Deficient Mutant ELOVL4 on Retinal Degeneration

Although our mutant and WT ELOVL4 constructs each caused RD in a similar proportion of animals, it is possible that the

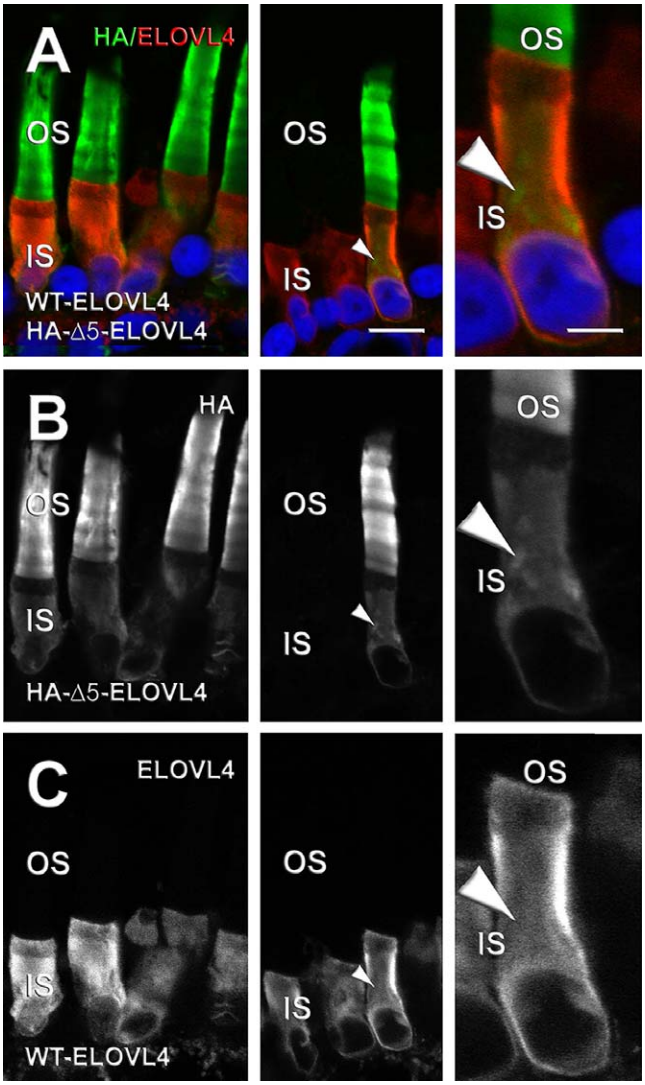

Figure 4. Effect of coexpression of HA-Δ5-ELOVL4 and WT ELOVL4 on mislocalization of WT ELOVL4 to photoreceptor OS. (**A**–**C**) Confocal micrographs of *X. laevis* rod photoreceptor cells coexpressing WT ELOVL4 (ELOVL4, *red*) and HA-Δ5-ELOVL4 (HA, *green*) with Hoescht 33342 (*blue*) ($n = 5$). WT ELOVL4 expression was restricted to IS without any OS localization (**A**, **C**), whereas HA-Δ5-ELOVL4 was distributed within IS and OS membranes (**A**, **B**). *White arrowheads* indicate internal IS membranes (likely Golgi) that are HA-positive and ELOVL4-negative. *Left* and *center* are from different transgenic retinas. *Right* shows higher magnification. *Scale bars*: 4 and 10 μm.

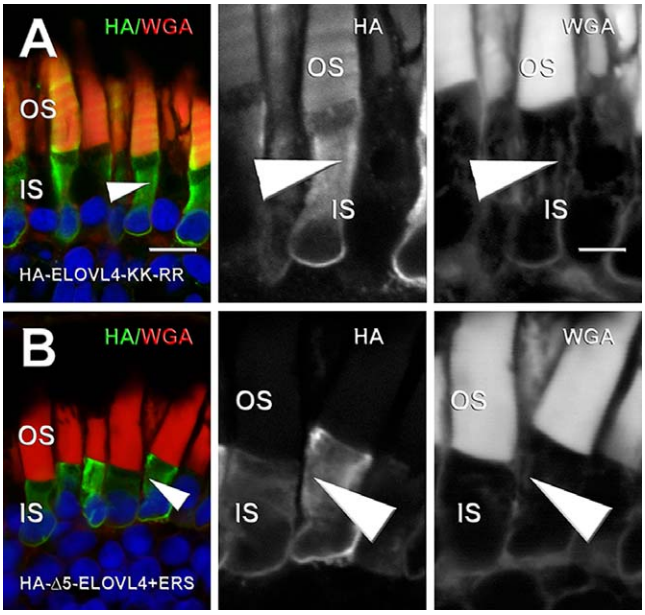

Figure 5. Role of the ELOVL4 KXKXX motif for inner segment targeting/retention of ELOVL4. (**A**) Confocal micrographs of transgenic *X. laevis* rod photoreceptors expressing HA-ELOVL4-KK-RR (HA: *green*, $n = 7$); note partial delocalization to OS membranes. *Arrowhead* indicates WGA-positive IS membranes. (**B**) Addition of KXKXX motif restores IS localization of HA-Δ5-ELOVL4 in transgenic *X. laevis* rod photoreceptors expressing HA-Δ5-ELOVL4-ERS (HA: *green*, $n = 8$). *Grayscale* shows the isolated WGA and HA signals. *Scale bars*: 10 μm.

underlying mechanisms differed between constructs. For example, it is possible that overexpression of HA-ELOVL4 caused cell death via ER stress, whereas overexpression of HA-Δ5-ELOVL4 caused cell death via a mechanism involving the enzymatic activity of ELOVL4 in inappropriate cellular compartments. Defects in fatty acid metabolism that result in generation of fatty acyl 3-keto intermediates (the product of ELOVL4) can cause cardiac and nervous system disorders.[45–47] For example, deficiency in breakdown of 3-keto-acyl CoA intermediates in trifunctional protein patients causes peripheral neuropathy.[45] Our cell culture studies showed that mutant ELOVL4 was not enzymatically active.[8] Although remote, it is still possible that HA-Δ5-ELOVL4 retains some condensation reaction activity in photoreceptor cells in the living retina. To address the possibility of generation of highly reactive 3-keto acyl-CoA intermediates within IS and OS membranes, we compared the effects of misrouting catalytically active and inactive mutant ELOVL4 on photoreceptors by mutating the critical dideoxy iron-binding motif HXXHH found within the catalytic core of most fatty acid elongase and desaturase enzymes to QXXQQ.[48] Both HA-Δ5-ELOVL4 and HA-Δ5-ELOVL4-3H3Q fusion proteins were misrouted to OS (Figs. 8A–C). Compared with control GFP-expressing transgenic animals (Fig. 8C) that do not develop RD, we did not observe a statistically significant reduction in total rhodopsin levels with either construct ($P = 0.45$, $n = 27$ per group, Kruskal-Wallace), although some RD was observed in histological sections (Figs. 7A–G). There was no observable difference in retinal structure or morphology in photoreceptors expressing HA-Δ5-ELOVL4 versus HA-Δ5-ELOVL4-3H3Q (Figs. 8B, 8C). The absence of any phenotypic differences supports our conclusion from cell culture studies that 3-keto acyl intermediates are not a factor in RD in our model of STGD3.[8]

Discussion

Here, we demonstrate that WT ELOVL4 is localized to the ER membranes of rod IS while truncated mutant ELOVL4 is prominently misrouted via the Golgi to OS disk membranes due to the absence of the KXKXX motif located in the C-terminal region. However, the mutant ELOVL4 does not demonstrate prominent plasma membrane, synaptic membrane, and OPL layer mislocalization as reported in heterozygous-knockin mice (*Elovl4*$^{+/stgd3}$).[18] We further demonstrate the absence of misrouting of WT ELOVL4 to OS via interaction with mutant ELOVL4. Previous cell culture studies suggest that mutant ELOVL4 may cause RD via a dominant negative effect, in which the mutant ELOVL4 interacts with and causes mislocalization and aggregate formation of the WT

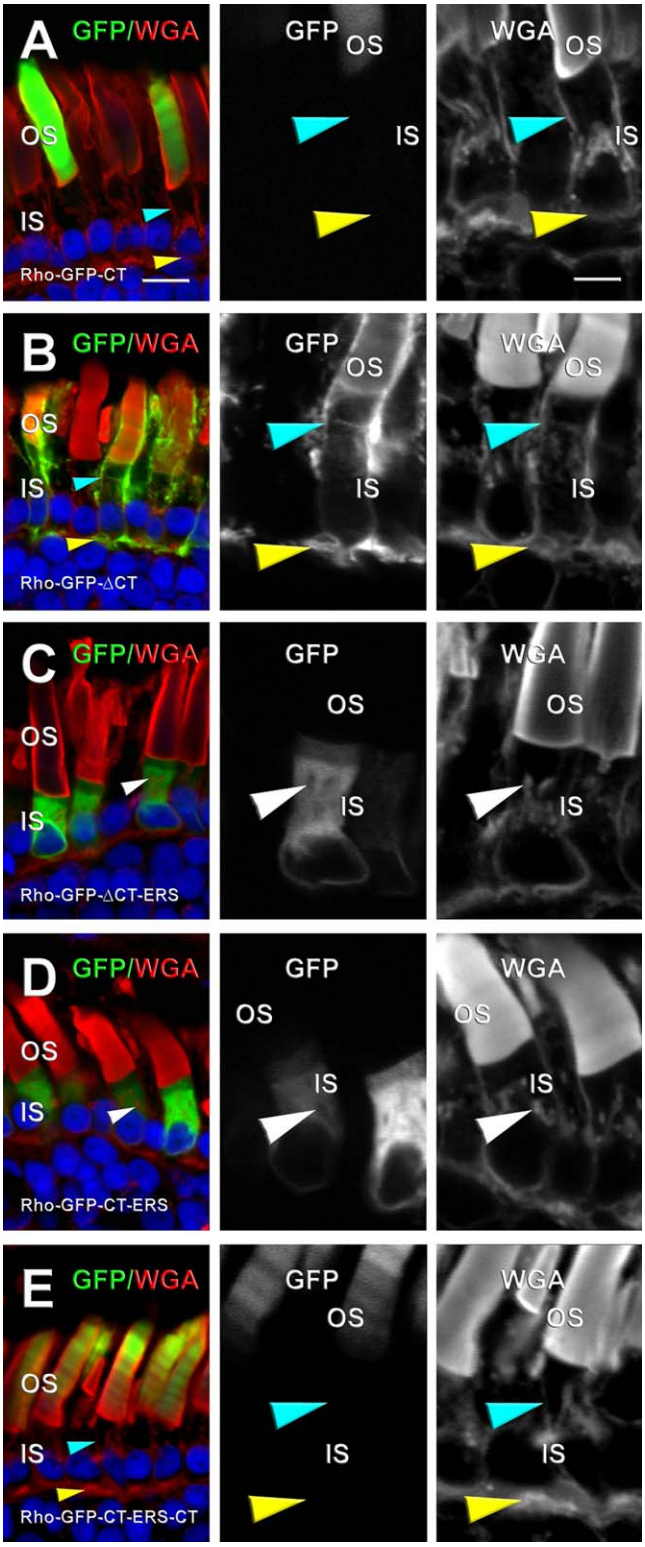

Figure 6. The ELOVL4 KXKXX motif can override OS targeting signals, provided it is located at the extreme carboxyl terminus. (**A**) Confocal micrograph of rod photoreceptors expressing Rho-GFP-CT (GFP: *green*, $n = 5$), which is primarily targeted to rod OS membranes due to presence of the rhodopsin OS targeting motif VXPX. There was no significant IS lateral plasma membrane (*blue arrow*) or synaptic region plasma membrane (*yellow arrow*) associated with Rho-GFP-CT. (**B**) Deletion of the rhodopsin OS targeting motif VXPX caused Rho-GFP-ΔCT signal (GFP: *green*, $n = 5$) to be distributed not only to OS, but also to the plasma membrane of the IS, including the lateral plasma membrane (*blue arrow*) and synaptic region plasma membrane (*yellow arrow*). (**C**, **D**) Addition of the last 12 amino acids containing the ER retention/retrieval signal of ELOVL4 to Rho-GFP-ΔCT and Rho-GFP-CT to generate Rho-GFP-ΔCT-ERS and Rho-GFP-CT-ERS fusion proteins (GFP: *green*, $n = 8$) resulted in complete and efficient IS retention and targeting of the fusion proteins. The fusion proteins were excluded from WGA-positive internal membranes (*white arrowheads*). (**E**) Rhodopsin OS targeting signal VXPX overrides the KXKXX motif when placed downstream of the KXKXX motif and directs Rho-GFP-CT-ERS-CT fusion protein (GFP: *green*, $n = 5$) to photoreceptor OS. No Rho-GFP-CT-ERS-CT fusion protein is retained within IS, including the lateral plasma membrane (*blue arrow*) or synaptic region membranes (*yellow arrow*). *Scale bars*: 10 μm (*color*) and 5 μm (*grayscale*).

ELOVL4.[4–8,37] However, our results do not support this mechanism. In *X. laevis* photoreceptors, WT ELOVL4 was retained within the ER and IS membranes without any evidence of being mislocalized to the OS via interaction with mutant ELOVL4. Furthermore, neither mutant nor WT ELOVL4 formed aggregates equivalent to those observed in cultured cells. Our results do not rule out the possibility that WT and mutant ELOVL4 may interact at a functional level within ER membranes, which may impact the biosynthetic ability of WT ELOVL4. However, with regard to sorting within photoreceptor cells, the localizations of WT and mutant ELOVL4 are independent of each other.

To understand the mechanism underlying the misrouting of the mutant ELOVL4 to photoreceptor OS, we expressed rhodopsin variants or mutant ELOVL4 fused to either the rhodopsin OS targeting signals or the ER targeting signal of ELOVL4. We demonstrate that the ELOVL4 ER retrieval/retention signal KXKXX is necessary and sufficient for constraining to the ER the localization of WT ELOVL4, mutant ELOVL4, and even OS-destined transmembrane proteins, such as a rhodopsin-GFP fusion protein. However, notably, the OS and post-Golgi compartments de-localization of mutant ELOVL4 does not precisely resemble the de-localization of mutant rhodopsin, lacking an OS localization signal in that some ER localization of mutant ELOVL4 persists. This is consistent with the KXKXX signal of ELOVL4 being a retention/retrieval signal recognized by receptors/coat proteins that reside/act in compartments distal to the ER, such as the ER-Golgi intermediate compartment and Golgi, where it promotes the recycling of ER-resident proteins that escape from the ER. Interestingly, unlike mislocalized rhodopsin Q344Ter, OS delocalized mutant ELOVL4 did not appear to be nonspecifically trafficked to the plasma membrane. This is in agreement with a previous study of ELOVL4 mutants in cultured cells in which mutant ELOVL4 accumulated in the Golgi or aggresomes of cultured cells without any plasma membrane labeling.[4–7,37]

Although the HA-Δ5-ELOVL4 and ELOVL4-K308/310R lacking the ER localization signal escape the Golgi and are delocalized to OS membranes, significant amounts of both were retained within IS membranes, including the ER. This suggests that, although absence of the KXKXX signal accounts for mislocalization of the mutant ELOVL4, other signals or interactions within the ELOVL4 also may contribute to retaining it within the ER. These signals or interactions also may play a role in preventing the mutant ELOVL4 from reaching the plasma membrane.[49] Indeed, ER retention motifs together with transmembrane-based retention signals have been described for several eukaryotic proteins.[50–53] For example, the human UDP-glucuronosyltranferase 1A (UGT1A) protein has both ER retention motif and transmembrane hydrophobic cores that retain the UGT1A within the ER.[52] Similarly, polar transmembrane-based amino acids are involved

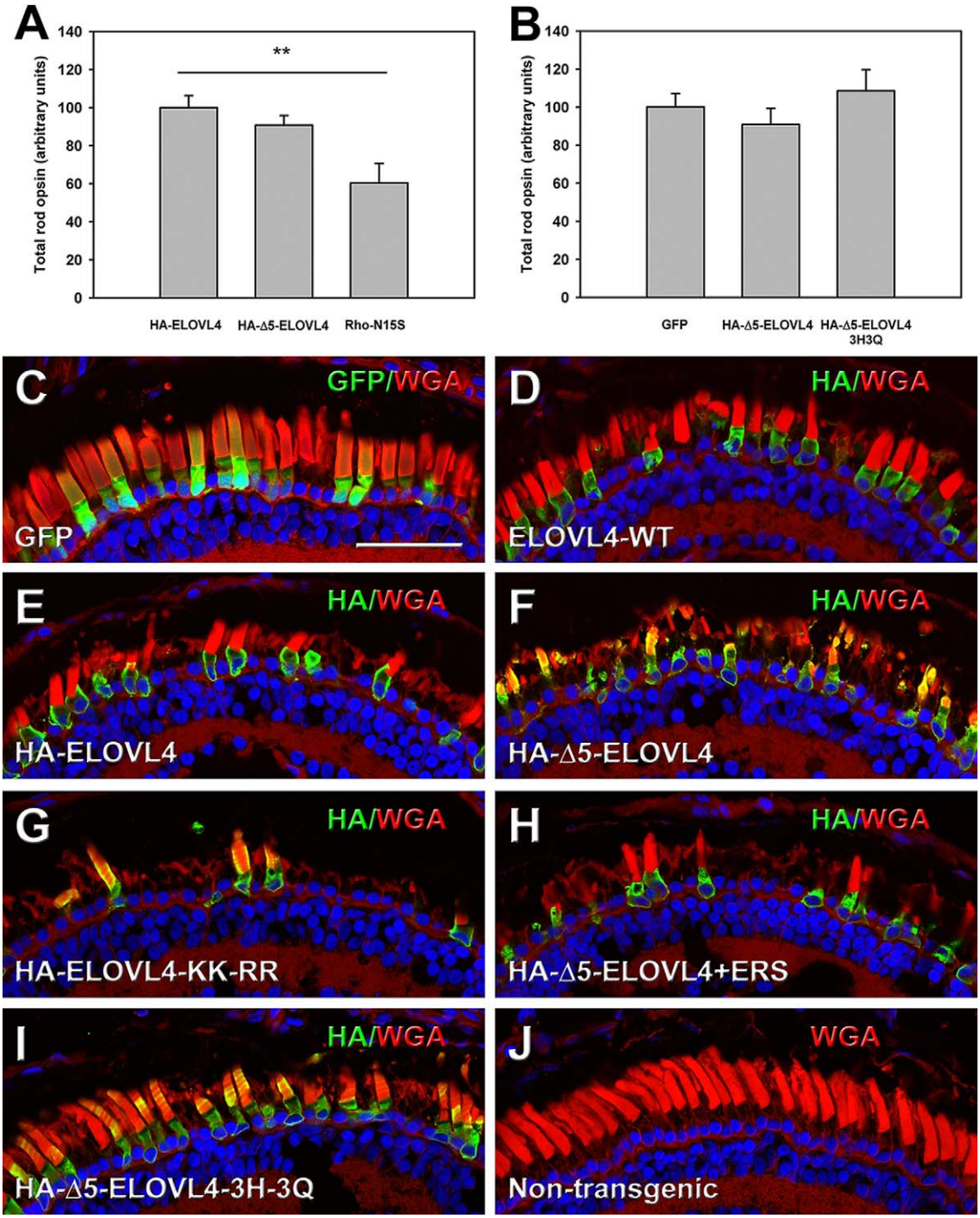

Figure 7. *ELOVL4* transgenes are relatively nontoxic, but occasionally induce RD in *X. laevis* retina. (**A**, **B**) Quantification of rod loss in HA-ELOVL4 versus HA-Δ5-ELOVL4 animals using a dot blot assay for rod opsin.[31] There was no statistically significant reduction in rod opsin in *X. laevis* expressing HA-ELOVL4 versus HA-Δ5-ELOVL4 (**A**), indicating that neither construct was dramatically more toxic than the other. In contrast, expression of N15S rhodopsin causes a significant decrease in total rod opsin relative to HA-ELOVL4 ($P = 0.008$, $n = 22$ per group, Kruskal-Wallace followed by multiple comparisons according to Conover[41]). (**B**) Quantification of rod loss in animals expressing GFP, HA-Δ5ELOVL4, and HA-Δ5ELOVL4-3H3Q using dot blot for rod opsin. GFP is a relatively nontoxic transgene product that does not cause retinal degeneration.[32] Total rod opsin levels are not significantly different between groups, indicating that HA-Δ5ELOVL4 and HA-Δ5ELOVL4-3H3Q are not significantly more toxic than GFP, or than each other, although a trend toward RD is apparent for HA-Δ5-ELOVL4 ($P = 0.45$, $n = 27$ per group, Kruskal-Wallace). (**C–J**) Expression of transgenic GFP (GFP: *green*, $n = 7$) (**C**) did not cause retinal degeneration and retained photoreceptor integrity similar to nontransgenics (**J**). However, occasionally retinas expressing ELOVL4 variants (**D–H**) had RD apparent by histology, as indicated by both loss of rods and shortened rod outer segments (n as reported in Figs. 1, 5, 8). *Scale bar*: 50 μm.

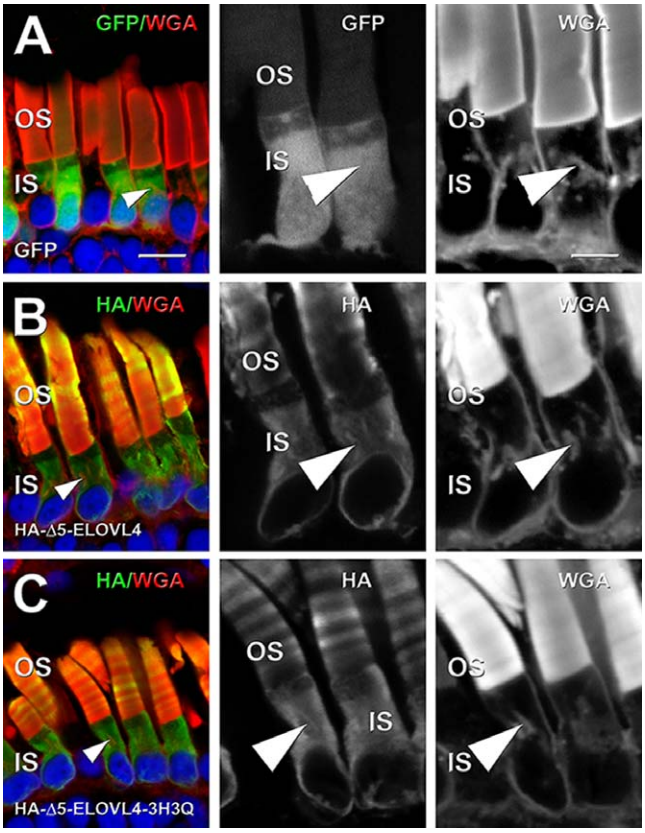

Figure 8. Localization of histidine-deficient mutant ELOVL4. (**A**) Transgenic expressed GFP protein (GFP: *green*, $n = 7$) is present throughout the IS, and at lower concentrations in OS. (**B**) Transgenically expressed HA-Δ5-ELOVL4 (HA: *green*, $n = 19$) and (**C**) HA-Δ5-ELOVL4-3H3Q HA: *green*, $n = 10$) fusion proteins were both localized to IS membranes, including WGA-positive internal membranes (*arrowheads*), and to photoreceptor OSs. *Scale bars*: 10 μm (merged) or 5 μm (*grayscale*).

in ER localization of presenilin 1.[50] Hence, there may be multiple signals that contribute to the localization of ELOVL4 to ER. It has been previously reported that proteins found exclusively in rod disks, such as peripherin/rds, rom-1, and ABCA4, are localized intracellularly when expressed in non-photoreceptor cell types.[54,55] However, to our knowledge, this is the first report of a normally intracellular protein adopting a disk-specific localization. This suggests that mechanisms involved in exclusion of proteins from the plasma membrane in other cell types also may be involved in segregating OS disk membrane proteins in photoreceptors. The exact mechanism by which mutant *ELOVL4* causes RD, however, remains elusive. We previously proposed three possibilities[8]:

1. Mutant protein generates toxic 3-keto-acyl intermediates that kill the cells,
2. Some important cellular function(s) is compromised by reduced levels of VLC-PUFA, or
3. Mislocalization of mutant protein causes cellular stress and/or interferes with important cellular functions.

The mutant ELOVL4 retains the histidine catalytic core motif (HXXHH) necessary for generating 3-keto-acyl fatty acids, the first and rate-limiting step in fatty acid elongation. The presence of this highly reactive fatty acid intermediate in the OS or other retinal membranes could potentially induce RD. However, cell culture studies in our laboratory show that the mutant ELOVL4 is not enzymatically active.[8] Also, in *X. laevis* retina, both HA-Δ5-ELOVL4-3H3Q and HA-Δ5-ELOVL4 constructs induced similar levels of RD. More importantly, coexpression of the HA-Δ5-ELOVL4 and WT ELOVL4 did not show an increase in RD, supporting the notion that the mutant ELOVL4 did not mislocalize the WT protein or, if it did, the WT did not synthesize toxic intermediates that destroyed retinal photoreceptors at 14 dpf. Thus, the *X. laevis* and cell culture studies do not support a role for toxic 3-keto-acyl intermediates generated by mutant ELOVL4 or by mislocalized WT ELOVL4 in the mechanism of RD in STGD3 macular dystrophy.[8] We do not, however, rule out the possibility of the mutant protein exerting a dominant negative effect on the VLC-PUFA biosynthetic activity of WT ELOVL4 within the photoreceptor IS as it transits through the ER, which would exacerbate the loss/reduction in retinal VLC-PUFA within photoreceptors, as reported in mice.[14]

A reduction in the function of WT ELOVL4 protein in the ER could result in a deficiency of VLC-PUFA, which may be required for the construction, function, and maintenance of healthy OS or other photoreceptor membranes; hence, the absence of sufficient quantities eventually results in retinal degeneration. This is supported by studies in knockin mice expressing one WT and one mutant copy of ELOVL4, showing that reduction of ELOVL4 in photoreceptors leads to reduction of retinal VLC-PUFA, which correlates with an age-dependent decline in photoreceptor function and structure.[11,14,18] However, results from conditional depletion of retinal VLC-PUFA have not been consistent. Barabas et al.[56] found no effect of VLC-PUFA reduction on rod or cone structure and function in mice, whereas Harkewicz et al.[57] found a loss of cone but not rod function in mice conditionally depleted of ELOVL4. Haploinsufficiency of ELOVL4 reduces levels of retinal VLC-PUFA by half,[19,20] as found in knockin mice,[14] but does not seem to cause RD. Thus, the studies to date using mouse models of STGD3 are inconclusive on the role of VLC-PUFA in the pathophysiology of this juvenile macular degeneration.

Our results clearly show mislocalization of mutant ELOVL4 and thus support the possibility that OS and Golgi delocalization of mutant ELOVL4 contributes to RD in STGD3 patients. The integrity of a photoreceptor membrane compartment could be compromised by the abnormal presence of mutant ELOVL4. This is likely the OS disks, but also could be a membrane compartment located between the ER and OS disks in the biosynthetic pathway, such as the Golgi, or even the retinal pigment epithelium. This could be due to nonspecific effects, such as a corresponding reduction in the density of rhodopsin within OS disk membranes, or the formation of abnormal hetero-oligomers with other OS membrane proteins, leading to alterations in membrane ultrastructure or biochemistry. Alternatively, membrane biochemistry may be directly altered by the abnormal presence of the mislocalized mutant ELOVL4. Other support for mislocalization being involved in the pathogenesis of STGD3 comes from the studies showing that heterozygous-knockin (*Elovl4*$^{+/stgd3}$), but not the heterozygous-knockout (*Elovl4*$^{\pm}$) have RD, albeit slow,[11,13,14,18] which is consistent with our findings that expression of the mutant ELOVL4 did not induce widespread RD in tadpoles, suggesting age-dependent onset or RD in STGD3. Also, the early studies of Karan et al.[10] showed that transgenic mice expressing mutant human ELOVL4 had RD that correlates with the level of transgene expression.

In conclusion, our studies clearly show that in *X. laevis*, mutant ELOVL4 is mislocalized to OS and Golgi membranes. WT ELOVL4 is confined to the IS membranes and is not mislocalized to OS or any IS membranes by interaction with mutant ELOVL4. A subset of the animals expressing mutant *ELOVL4* transgenes developed RD, suggesting that expression of the mutant ELOVL4 contributes to RD; however, it is not

clear that this occurred via mechanisms common to STGD3 patients. This question will require further investigation and comparison of transgenic animal phenotypes and STGD3 phenotypes.

Acknowledgments

We thank Steve Brush for his useful comments and suggestions.

Supported by grants from Hope for Vision and Knight Templar Eye Foundation, Inc. (MPA); the National Institutes of Health (EY04149, EY00871, EY021725, and RR17703), Research to Prevent Blindness, Inc., and the Foundation Fighting Blindness (REA); and Foundation Fighting Blindness-Canada and the Canadian Institutes of Health Research (MOP-64400) (OLM).

Disclosure: **M.-P. Agbaga**, P; **B.M. Tam**, None; **J.S. Wong**, None; **L.L. Yang**, None; **R.E. Anderson**, P; **O.L. Moritz**, None

References

1. Zhang K, Kniazeva M, Han M, et al. A 5-bp deletion in ELOVL4 is associated with two related forms of autosomal dominant macular dystrophy. *Nat Genet*. 2001;27:89–93.
2. Agbaga MP, Brush RS, Mandal MN, Elliott MH, Al-Ubaidi MR, Anderson RE. Role of elovl4 protein in the biosynthesis of docosahexaenoic acid. *Adv Exp Med Biol*. 2010;664:233–242.
3. Carmona-Antonanzas G, Monroig O, Dick JR, Davie A, Tocher DR. Biosynthesis of very long-chain fatty acids (C>24) in Atlantic salmon: cloning, functional characterisation, and tissue distribution of an Elovl4 elongase. *Comp Biochem Physiol B Biochem Mol Biol*. 2011;159:122–129.
4. Ambasudhan R, Wang X, Jablonski MM, et al. Atrophic macular degeneration mutations in ELOVL4 result in the intracellular misrouting of the protein. *Genomics*. 2004;83:615–625.
5. Karan G, Yang Z, Zhang K. Expression of wild type and mutant ELOVL4 in cell culture: subcellular localization and cell viability. *Mol Vis*. 2004;10:248–253.
6. Vasireddy V, Vijayasarathy C, Huang J, et al. Stargardt-like macular dystrophy protein ELOVL4 exerts a dominant negative effect by recruiting wild-type protein into aggresomes. *Mol Vis*. 2005;11:665–676.
7. Grayson C, Molday RS. Dominant negative mechanism underlies autosomal dominant Stargardt-like macular dystrophy linked to mutations in ELOVL4. *J Biol Chem*. 2005;280:32521–32530.
8. Logan S, Agbaga MP, Chan MD, et al. Deciphering mutant ELOVL4 activity in autosomal-dominant Stargardt macular dystrophy. *Proc Natl Acad Sci U S A*. 2013;110:5446–5451.
9. Tam BM, Moritz OL. Characterization of rhodopsin P23H-induced retinal degeneration in a *Xenopus laevis* model of retinitis pigmentosa. *Invest Ophthalmol Vis Sci*. 2006;47:3234–3241.
10. Karan G, Lillo C, Yang Z, et al. Lipofuscin accumulation, abnormal electrophysiology, and photoreceptor degeneration in mutant ELOVL4 transgenic mice: a model for macular degeneration. *Proc Natl Acad Sci U S A*. 2005;102:4164–4169.
11. Vasireddy V, Jablonski MM, Mandal MN, et al. Elovl4 5-bp-deletion knock-in mice develop progressive photoreceptor degeneration. *Invest Ophthalmol Vis Sci*. 2006;47:4558–4568.
12. Vasireddy V, Uchida Y, Salem N Jr, et al. Loss of functional ELOVL4 depletes very long-chain fatty acids (> or =C28) and the unique omega-O-acylceramides in skin leading to neonatal death. *Hum Mol Genet*. 2007;16:471–482.
13. McMahon A, Butovich IA, Mata NL, et al. Retinal pathology and skin barrier defect in mice carrying a Stargardt disease-3 mutation in elongase of very long chain fatty acids-4. *Mol Vis*. 2007;13:258–272.
14. McMahon A, Jackson SN, Woods AS, Kedzierski WA. Stargardt disease-3 mutation in the mouse Elovl4 gene causes retinal deficiency of C32-C36 acyl phosphatidylcholines. *FEBS Lett*. 2007;581:5459–5463.
15. Lagali PS, Liu J, Ambasudhan R, et al. Evolutionarily conserved ELOVL4 gene expression in the vertebrate retina. *Invest Ophthalmol Vis Sci*. 2003;44:2841–2850.
16. Agbaga MP, Brush RS, Mandal MN, Henry K, Elliott MH, Anderson RE. Role of Stargardt-3 macular dystrophy protein (ELOVL4) in the biosynthesis of very long chain fatty acids. *Proc Natl Acad Sci U S A*. 2008;105:12843–12848.
17. Sommer JR, Estrada JL, Collins EB, et al. Production of ELOVL4 transgenic pigs: a large animal model for Stargardt-like macular degeneration. *Br J Ophthalmol*. 2011;95:1749–1754.
18. Vasireddy V, Jablonski MM, Khan NW, et al. Elovl4 5-bp deletion knock-in mouse model for Stargardt-like macular degeneration demonstrates accumulation of ELOVL4 and lipofuscin. *Exp Eye Res*. 2009;89:905–912.
19. Raz-Prag D, Ayyagari R, Fariss RN, et al. Haploinsufficiency is not the key mechanism of pathogenesis in a heterozygous Elovl4 knockout mouse model of STGD3 disease. *Invest Ophthalmol Vis Sci*. 2006;47:3603–3611.
20. Li W, Chen Y, Cameron DJ, et al. Elovl4 haploinsufficiency does not induce early onset retinal degeneration in mice. *Vision Res*. 2007;47:714–722.
21. Tam BM, Xie G, Oprian DD, Moritz OL. Mislocalized rhodopsin does not require activation to cause retinal degeneration and neurite outgrowth in *Xenopus laevis*. *J Neurosci*. 2006;26:203–209.
22. Tam BM, Lai CC, Zong Z, Moritz OL. Generation of transgenic *X. laevis* models of retinal degeneration. *Methods Mol Biol*. 2013;935:113–125.
23. Tam BM, Moritz OL, Hurd LB, Papermaster DS. Identification of an outer segment targeting signal in the COOH terminus of rhodopsin using transgenic *Xenopus laevis*. *J Cell Biol*. 2000;151:1369–1380.
24. Amaya E, Kroll KL. A method for generating transgenic frog embryos. *Methods Mol Biol*. 1999;97:393–414.
25. Moritz OL, Biddle KE, Tam BM. Selection of transgenic *Xenopus laevis* using antibiotic resistance. *Transgenic Res*. 2002;11:315–319.
26. Chedid A, Mendenhall CL, Moritz TE, et al. Cell-mediated hepatic injury in alcoholic liver disease. Veterans Affairs Cooperative Study Group 275. *Gastroenterology*. 1993;105:254–266.
27. Tam BM, Moritz OL. Dark rearing rescues P23H rhodopsin-induced retinal degeneration in a transgenic *Xenopus laevis* model of retinitis pigmentosa: a chromophore-dependent mechanism characterized by production of N-terminally truncated mutant rhodopsin. *J Neurosci*. 2007;27:9043–9053.
28. Lee DC, Vazquez-Chona FR, Ferrell WD, et al. Dysmorphic photoreceptors in a P23H mutant rhodopsin model of retinitis pigmentosa are metabolically active and capable of regenerating to reverse retinal degeneration. *J Neurosci*. 2012;32:2121–2128.
29. Hicks D, Molday RS. Differential immunogold-dextran labeling of bovine and frog rod and cone cells using monoclonal antibodies against bovine rhodopsin. *Exp Eye Res*. 1986;42:55–71.
30. Adamus G, Zam ZS, Arendt A, Palczewski K, McDowell JH, Hargrave PA. Anti-rhodopsin monoclonal antibodies of defined specificity: characterization and application. *Vision Res*. 1991;31:17–31.
31. Tam BM, Moritz OL. The role of rhodopsin glycosylation in protein folding, trafficking, and light-sensitive retinal degeneration. *J Neurosci*. 2009;29:15145–15154.
32. Moritz OL, Tam BM, Knox BE, Papermaster DS. Fluorescent photoreceptors of transgenic *Xenopus laevis* imaged in vivo

by two microscopy techniques. *Invest Ophthalmol Vis Sci*. 1999;40:3276–3280.

33. Baker SA, Haeri M, Yoo P, et al. The outer segment serves as a default destination for the trafficking of membrane proteins in photoreceptors. *J Cell Biol*. 2008;183:485–498.
34. Moritz OL, Tam BM, Papermaster DS, Nakayama T. A functional rhodopsin-green fluorescent protein fusion protein localizes correctly in transgenic *Xenopus laevis* retinal rods and is expressed in a time-dependent pattern. *J Biol Chem*. 2001; 276:28242–28251.
35. Logan S, Agbaga MP, Chan MD, Brush RS, Anderson RE. Endoplasmic reticulum microenvironment and conserved histidines govern ELOVL4 fatty acid elongase activity. *J Lipid Res*. 2014;55:698–708.
36. Mazelova J, Astuto-Gribble L, Inoue H, et al. Ciliary targeting motif VxPx directs assembly of a trafficking module through Arf4. *EMBO J*. 2009;28:183–192.
37. Karan G, Yang Z, Howes K, et al. Loss of ER retention and sequestration of the wild-type ELOVL4 by Stargardt disease dominant negative mutants. *Mol Vis*. 2005;11:657–664.
38. Luo W, Marsh-Armstrong N, Rattner A, Nathans J. An outer segment localization signal at the C terminus of the photoreceptor-specific retinol dehydrogenase. *J Neurosci*. 2004;24:2623–2632.
39. Jackson MR, Nilsson T, Peterson PA. Identification of a consensus motif for retention of transmembrane proteins in the endoplasmic reticulum. *EMBO J*. 1990;9:3153–3162.
40. Deretic D, Schmerl S, Hargrave PA, Arendt A, McDowell JH. Regulation of sorting and post-Golgi trafficking of rhodopsin by its C-terminal sequence QVS(A)PA. *Proc Natl Acad Sci U S A*. 1998;95:10620–10625.
41. Conover WJ. Practical nonparametric statistics. 3rd ed. New York: Wiley; 1999.
42. Haeri M, Knox BE. Rhodopsin mutant P23H destabilizes rod photoreceptor disk membranes. *PLoS ONE*. 2012;7:e30101.
43. Moritz OL, Tam BM. Recent insights into the mechanisms underlying light-dependent retinal degeneration from *X. laevis* models of retinitis pigmentosa. *Adv Exp Med Biol*. 2010;664: 509–515.
44. Tam BM, Qazalbash A, Lee HC, Moritz OL. The dependence of retinal degeneration caused by the rhodopsin P23H mutation on light exposure and vitamin a deprivation. *Invest Ophthalmol Vis Sci*. 2010;51:1327–1334.
45. Roe CR, Roe DS, Wallace M, Garritson B. Choice of oils for essential fat supplements can enhance production of abnormal metabolites in fat oxidation disorders. *Mol Genet Metab*. 2007;92:346–350.
46. Kimura I, Inoue D, Maeda T, et al. Short-chain fatty acids and ketones directly regulate sympathetic nervous system via G protein-coupled receptor 41 (GPR41). *Proc Natl Acad Sci U S A*. 2011;108:8030–8035.
47. Bank IM, Shemie SD, Rosenblatt B, Bernard C, Mackie AS. Sudden cardiac death in association with the ketogenic diet. *Pediatr Neurol*. 2008;39:429–431.
48. Chertemps T, Duportets L, Labeur C, et al. A female-biased expressed elongase involved in long-chain hydrocarbon biosynthesis and courtship behavior in *Drosophila melanogaster*. *Proc Natl Acad Sci U S A*. 2007;104:4273–4278.
49. Li Q, Su YY, Wang H, Li L, Wang Q, Bao L. Transmembrane segments prevent surface expression of sodium channel Nav1.8 and promote calnexin-dependent channel degradation. *J Biol Chem*. 2010;285:32977–32987.
50. Fassler M, Li X, Kaether C. Polar transmembrane-based amino acids in presenilin 1 are involved in endoplasmic reticulum localization, Pen2 protein binding, and gamma-secretase complex stabilization. *J Biol Chem*. 2011;286:38390–38396.
51. Kaether C, Scheuermann J, Fassler M, et al. Endoplasmic reticulum retention of the gamma-secretase complex component Pen2 by Rer1. *EMBO Rep*. 2007;8:743–748.
52. Barre L, Magdalou J, Netter P, Fournel-Gigleux S, Ouzzine M. The stop transfer sequence of the human UDP-glucuronosyltransferase 1A determines localization to the endoplasmic reticulum by both static retention and retrieval mechanisms. *FEBS J*. 2005;272:1063–1071.
53. Beaudoin F, Napier JA. Targeting and membrane-insertion of a sunflower oleosin in vitro and in *Saccharomyces cerevisiae*: the central hydrophobic domain contains more than one signal sequence, and directs oleosin insertion into the endoplasmic reticulum membrane using a signal anchor sequence mechanism. *Planta*. 2002;215:293–303.
54. Goldberg AF, Moritz OL, Molday RS. Heterologous expression of photoreceptor peripherin/rds and Rom-1 in COS-1 cells: assembly, interactions, and localization of multisubunit complexes. *Biochemistry*. 1995;34:14213–14219.
55. Zhong M, Molday LL, Molday RS. Role of the C terminus of the photoreceptor ABCA4 transporter in protein folding, function, and retinal degenerative diseases. *J Biol Chem*. 2009;284: 3640–3649.
56. Barabas P, Liu A, Xing W, et al. Role of ELOVL4 and very long-chain polyunsaturated fatty acids in mouse models of Stargardt type 3 retinal degeneration. *Proc Natl Acad Sci U S A*. 2013; 110:5181–5186.
57. Harkewicz R, Du H, Tong Z, et al. Essential role of ELOVL4 protein in very long chain fatty acid synthesis and retinal function. *J Biol Chem*. 2012;287:11469–11480.

Investigative Ophthalmology & Visual Science